

FIG. 2. Herman's most recent results for the energy band structure of Ge along principal directions.

crystal is given by a superposition of spherically symmetric neutral atomic charge densities, with $r=0$ at the nucleus in an atomic cell, then

$$V_{000} = \frac{16\pi^2}{3\Omega_0} \int_0^\infty \rho(r)r^4 dr \quad (2.1)$$

gives the zero of energy for valence electrons in a monatomic lattice. Here Ω_0 is the atomic volume and $\rho(r)$ is the atomic charge density. Because of the extremely anisotropic unit cell in tetrahedrally coordinated lattices, it has so far proved necessary to calculate energy bands using the orthogonalized plane-wave method, which treats valence and core states separately. The zero of energy for core states is taken to be the same as in the free atom; then the core energies $E_{n\alpha}$ are easily determined.

In this formalism the repulsive orthogonality terms are proportional to

$$(E_k + V_{000} - E_{n\alpha}), \quad (2.2)$$

where E_k is a valence eigenvalue. As a result, as Herman has emphasized,¹⁰ certain energy levels are extremely sensitive to $E_{n\alpha}$ and V_{000} . One may alter (2.2) either by varying V_{000} or by shifting all $E_{n\alpha}$ by ΔE_c . Here ΔE_c is, in Herman's nomenclature, a "core shift" which changes (2.2) without shifting the valence zero of energy. Herman's results for Ge at Γ and L are shown in Fig. 3.

Herman has chosen to vary ΔE_c or V_{000} , which is difficult to calculate from (2.1), to obtain bands in agreement with experiment at Γ , X , and L . The bands shown in Fig. 2 are the successful product of this approach. In Ge Herman uses $\Delta E_c = -3.0$ ry, a rather large shift.

An interesting feature of Fig. 3 is that the levels are divided into two classes. The levels Γ_{15} , $L_{3'}$, L_3 , X_4 , X_1 all move parallel to $\Gamma_{25'}$, which we shall use to fix the zero of energy. (Although Herman gives results for X , these are omitted from Fig. 3.) The s levels $\Gamma_{2'}$ and L_1

vary much more rapidly with V_{000} , $\Gamma_{2'}$ shifting about twice as fast as L_1 . These features are extremely suggestive, since we shall see in Sec. 3 that this is the way energy levels change with pressure and alloying of Ge and Si.

Because V_{000} is difficult to obtain, theoretical estimates of energy gaps among levels belonging to the first class are expected to be more reliable. Thus for $X_1 - \Gamma_{25'}$, Kleinman and Phillips⁶ found 0.10 ry, as compared to Woodruff's⁵ 0.35 ry and the experimental value 0.08 ry. On the other hand, we shall see that the positions assigned $\Gamma_{2'}$ and L_1 in reference 6 differ very substantially from the experimental values.

We therefore propose to correlate the band structures of Si and Ge using only V_{000} . However, our treatment should not be taken too literally. For reasons of cohesive energy V_{000} is probably about the same in each crystal. What changes is E_{ns} and E_{np} , the energies of the $2s$ and $2p$ levels in Si relative to the $3s$ and $3p$ levels in Ge. Because the $3d$ electrons in Ge lie somewhat outside the $3s$ and $3p$ electrons, E_{3s}^{Ge} and E_{3p}^{Ge} are somewhat more negative than E_{2s}^{Si} and E_{2p}^{Si} , respectively. According to (2.2) this core shift can also be represented by changes in V_{000} .

Before proceeding to the experimental data we must discuss the calculation of matrix elements which are important in estimating effective masses. In view of the uncertainty in energy levels it might appear that little confidence can be placed in calculated matrix elements. Actually, matrix elements between levels of high symmetry are probably much more accurate than energy differences.

The reason for this can be seen by a simple example. Consider the wave functions (\mathbf{K} is a reciprocal lattice vector)

$$\psi_e = \frac{1}{\sqrt{2}}(e^{\frac{1}{2}i\mathbf{K}\cdot\mathbf{r}} + e^{-\frac{1}{2}i\mathbf{K}\cdot\mathbf{r}}), \quad (2.3)$$

$$\psi_0 = \frac{1}{\sqrt{2}}(e^{\frac{1}{2}i\mathbf{K}\cdot\mathbf{r}} - e^{-\frac{1}{2}i\mathbf{K}\cdot\mathbf{r}}), \quad (2.4)$$

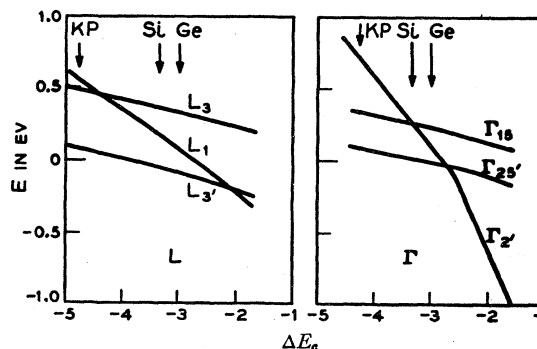


FIG. 3. The variation of important valence and conduction band levels in Ge as a function of ΔE_c (in rydbergs), according to Herman. "KP" and "Ge" mark the positions of the levels in Figs. 1 and 2, respectively, while "Si" gives the levels of Si as deduced here from experiment.

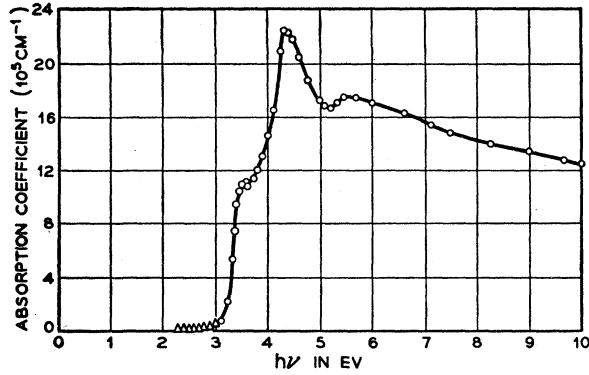


FIG. 4. The spectral dependence of the absorption coefficient of Si, according to Philipp and Taft.

with $E_e = E + V_K$, $E_0 = E - V_K$. The matrix element

$$M^2 \sim |\langle \psi_e | \mathbf{p} | \psi_0 \rangle|^2 = \hbar^2 K^2 / 4 \quad (2.5)$$

is independent of $E_e - E_0 = 2V_K$. Only when one mixes ψ_e^n with $\psi_e^{n'}$ will M^2 be changed. At points of high symmetry such as Γ , X , and L , $E_e^{n'} - E_e^n \sim \hbar^2 K^2 / 2m \sim 1$ ry. Shifting an energy level by 1 ev alters matrix elements by about 10% or less.

According to the last paragraph if energy levels shift by only a few ev from one semiconductor to another, the approximate constancy of matrix elements can be used to estimate energy differences from effective mass data. In changing crystals we change atomic cores. Because of the cancellation of repulsive orthogonalization terms and core potentials^{11,12} we are not surprised that the shifts are small.

Some mention must be made of the effect of orthogonalization corrections on matrix elements, e.g.,

$$M_{F^2}^2 \sim |\langle \Gamma_{2'} | \mathbf{p} | \Gamma_{25'} \rangle|^2. \quad (2.6)$$

Because of the symmetry of $\Gamma_{2'}$ and $\Gamma_{25'}$, we may write to a good approximation

$$\Gamma_{2'} > = \frac{1}{(1-a^2)^{1/2}} (\Phi_s - a\psi_s). \quad (2.7)$$

$$\Gamma_{25'} > = \frac{1}{(1-b^2-c^2)^{1/2}} (\Phi_p - b\psi_p - c\psi_d). \quad (2.8)$$

Here Φ is the "smooth" part of the wave function, made out of symmetrized combinations of plane waves, and ψ_s , ψ_p , and ψ_d are the atomic wave functions in the last shell of the core. The argument following (2.5) applied only to

$$(M_{F'})^2 \sim |\langle \Phi_s | \mathbf{p} | \Phi_p \rangle|^2. \quad (2.9)$$

However, in silicon the extra terms were found⁶ to change M_{F^2} by less than 20%. Moreover, ψ_s , ψ_p , and ψ_d vary little from one row of the periodic table to

another, as long as that level is actually available in the core. In Si, however, $c=0$ and this should account for much of the variation in M_{F^2} from Si to Ge. Even this contribution is small, however, since in Ge c is much smaller than a or b .

3. EXPERIMENTAL EVIDENCE

Two recent experiments have shed new light on the band structure of Si. Tauc and Abraham^{13,14} have studied optical absorption in Ge-Si alloys from 1 to 5 ev. The absorption edges of Ge remain well defined and shift linearly with Si content until 80% Si. The first large absorption edge,¹⁵ which started at 2.1 ev in Ge and which extrapolates to 3.6 ev in Si, breaks at this point. Presumably this is due to the new band edge at 3.4 ev in Si. The absorption of Si is shown¹⁶⁻¹⁸ in Fig. 4.

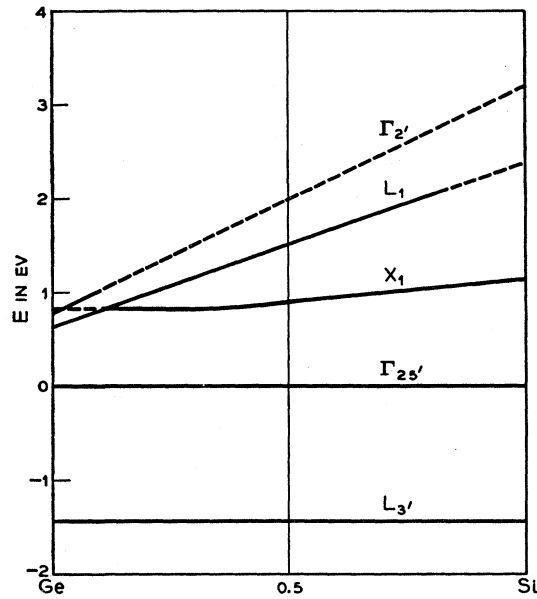


FIG. 5. The variation of important valence and conduction band levels in Ge-Si alloys. The solid lines are taken from observed absorption edges, while the dashed lines are extrapolations of the solid lines.

¹³ J. Tauc and A. Abraham, see reference 10.

¹⁴ J. Tauc and A. Abraham, *J. Phys. Chem. Solids* **20**, 190 (1961).

¹⁵ H. R. Philipp and E. A. Taft, *Phys. Rev.* **113**, 1002 (1959).

¹⁶ H. R. Philipp and E. A. Taft, *Phys. Rev.* **120**, 37 (1960).

¹⁷ The structure in the imaginary part of the dielectric constant (see Fig. 6 in reference 15), which is proportional to the conductivity, reflects more accurately direct transition edges. However, qualitatively the same edges are present in both cases. Cardona and Sommers, in reference 18, suggest, on the basis of a two-band model for the dielectric constant, that direct transition edges are to be identified only with maxima in the real part of the dielectric constant. We cannot agree with this statement in the case of complex band structures, where we feel that edges in the conductivity provide better evidence for the existence of direct transition edges. It should also be noted that much of the structure in Fig. 6 of reference 15 has been smoothed out in the plot of the real and imaginary parts of the dielectric constant in Fig. 7 of reference 18.

¹⁸ M. Cardona and H. S. Sommers, Jr., *Phys. Rev.* **122**, 1382 (1961).

¹¹ J. C. Phillips and L. Kleinman, *Phys. Rev.* **116**, 287 (1959).

¹² M. H. Cohen and V. Heine, *Phys. Rev.* **122**, 1821 (1961).

Some of Tauc's results, together with earlier work¹⁹ on the indirect and direct absorption edges, are shown in Fig. 5.

In Fig. 5 we have extrapolated several edges which are observable over concentration ranges of little more than 10%. Consider, e.g., $\Gamma_{25'} \rightarrow L_1$ and $L_{3'} \rightarrow L_1$. (Because of spin-resonance g values, this transition has been identified^{20,21} in Ge.) While the latter is observed from 0–80% the former is seen only for 0–15% Si. On the assumption that $L_{3'}$ does not move relative to $\Gamma_{25'}$, both lines extrapolate to $L_1=3.6$ ev in Si. Similarly, $\Gamma_{2'}$ extrapolates to 3.2 ev.

The original cyclotron resonance experiments on p -type Ge and Si yielded values for A , $|B|$, and C , where

$$A = 1 + \frac{1}{3}(F + 2G + 2H_1), \quad (3.1)$$

$$3B = F + 2G - H_1, \quad (3.2)$$

$$3C^2 = N^2 - (3B^2), \quad (3.3)$$

$$N = F - G + H_1. \quad (3.4)$$

Here F , G , and H_1 are given by

$$F = \frac{\hbar^2}{2m} \frac{|\langle \Gamma_{2'} | p | \Gamma_{25'} \rangle|^2}{E_0 - E_1}, \quad (3.5)$$

$$G = \frac{\hbar^2}{2m} \frac{|\langle \Gamma_{12'} | p | \Gamma_{25'} \rangle|^2}{E_0 - E_2}, \quad (3.6)$$

$$H_1 = \frac{\hbar^2}{2m} \frac{|\langle \Gamma_{15} | p | \Gamma_{25'} \rangle|^2}{E_0 - E_3}, \quad (3.7)$$

and E_0, E_1, E_2, E_3 refer to the energies of $\Gamma_{25'}, \Gamma_{2'}, \Gamma_{12'}$, and Γ_{15} in Figs. 1 and 2. The contributions of higher bands of the same symmetry and also a higher Γ_{25} band have been omitted, since these were found to be very small in reference 6.

Because of the threefold degeneracy of $\Gamma_{25'}$ levels, these experiments yielded only $|B|$. In Si two sets of values of F , G , and H_1 could then be obtained. Feher and Hensel²² and Hensel²³ have studied cyclotron resonances in strained p -type Si which determine the sign of B and yield more accurate values of A , B , and N :

$$A = -4.28 \pm 0.02, \quad B = -0.75 \pm 0.05, \quad (3.8)-(3.10)$$

$$N = -9.36 \pm 0.10.$$

From (3.8)–(3.10) we find for Si

$$F = -5.4, \quad G = -0.7, \quad H_1 = -4.5, \quad (3.11)$$

in qualitative agreement with Dresselhaus,³ as corrected

in reference 4. According to the discussion of Sec. 2, the matrix elements calculated in reference 6 can now be used to give

$$E_0 - E_1 \sim 2.8 \text{ ev}, \quad E_0 - E_2 \sim 10 \text{ ev}, \quad (3.12)$$

$$E_0 - E_3 = 2.8 \text{ ev}.$$

In reference 6 energy differences of 2.1, 10, and 8.8 ev, respectively, were used. The value of E_1 given by (3.12) is in good agreement with that estimated in Fig. 5.

Returning to Fig. 3, we now see that L_1 and $\Gamma_{2'}$ levels in Si as deduced here can be obtained by extrapolating Herman's results for Ge. Extrapolating still further, we obtain the level scheme of Si as calculated in reference 6. Furthermore, the positions of L_1 (3.6 ev) and $\Gamma_{2'}$ (3 ev) in Si have each been deduced by two separate indirect arguments. The value of ΔE_c required to give Kleinman and Phillips' $\Gamma_{2'}$ (−4.2 ry) is quite close to that required for their L_1 (−4.6 ry).

To complete the classification of energy levels in Si and Ge it is necessary to identify the peaks in optical absorption in Si (A , 4.3 ev; B , 5.4 ev) and Ge (A , 4.4 ev; B , 5.8 ev). We estimate A to be 4 to 5 times stronger than B in each crystal. We must also identify C , the 3.4-ev edge in Si.

Previously it was tentatively suggested²¹ that A was due to $X_4 \rightarrow X_1$ transitions. Tauc has suggested¹⁴ $L_{3'} \rightarrow L_3$ for C . We have several useful guides here. According to Elliott²⁴ the strength of an optical absorption edge is proportional to

$$K \sim \nu \mu^2 x^2, \quad (3.13)$$

where ν is the frequency and μ the density-of-states reduced effective mass. Here x is a matrix element which we take to be the same for allowed $X_4 \rightarrow X_1$ and $L_{3'} \rightarrow L_3$ transitions.

The second guide is that $L_{3'}$, L_3 , X_4 , and X_1 belong to the "insensitive" levels in Fig. 3. Thus some confidence can be placed in the theoretical energy differences given there ($L_{3'} \rightarrow L_3 = 6$ ev, $X_4 \rightarrow X_1 = 5$ ev).

Thus it is quite probable that A and B belong to $X_4 \rightarrow X_1$ and $L_{3'} \rightarrow L_3$. A definitive pairing is suggested by (3.13). Since L_1 is now about 3 ev from $L_{3'}$ and L_3 , μ_i for these levels is of the order of m_i for L_1 (0.08 m) as compared to $\frac{1}{2}m_i$ for X_1 and X_4 (0.10 m). Also μ_i is much smaller at L because of the repulsion of $L_{3'}$ and L_3 . Moreover, twice as many transitions are allowed near X ($\Delta_5 \rightarrow \Delta_1, \Delta_2'$) as near L . Thus the original assignment of A to $X_4 \rightarrow X_1$ appears to be satisfactory; B is assigned to $L_{3'} \rightarrow L_3$.

The levels L_3 and $L_{3'}$ are split by spin-orbit interaction, while X_1 and X_4 are not.³ If the L_3 and $L_{3'}$ spin-orbit splittings are equal, as suggested by the tight-binding approximation group theory³ shows that three edges, of strength 1:2:1, should be observed for $L_{3'} \rightarrow L_3$. High-resolution studies¹⁸ of A reveal no

¹⁹ R. Braunstein, A. R. Moore, and F. Herman, Phys. Rev. **109**, 695 (1958).

²⁰ L. M. Roth and B. Lax, Phys. Rev. Letters **3**, 217 (1959).

²¹ J. C. Phillips, J. Phys. Chem. Solids **12**, 208 (1960).

²² G. Feher and J. C. Hensel, Phys. Rev. Letters **5**, 307 (1960).

²³ J. C. Hensel (private communication).

²⁴ R. J. Elliott, Phys. Rev. **108**, 1383 (1957).

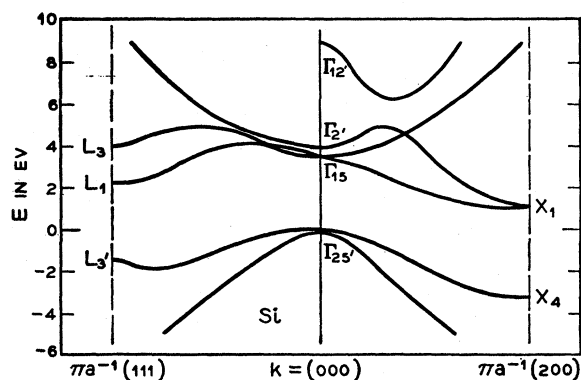


FIG. 6. A sketch of the energy bands of silicon near the energy gap, as deduced from the experimental data discussed in this paper. Note that the "insensitive" levels in Fig. 3 are given correctly by Fig. 1.

The sensitive levels $\Gamma_{2'}$ and L_1 are shifted from the values of Fig. 1 (marked "KP" in Fig. 3) to the values marked "Si" in Fig. 3.

structure, although the expected structure for $L_{3'} \rightarrow L_1$ is well resolved. Again, A must be $X_4 \rightarrow X_1$. Edge B , which we have assigned to $L_{3'} \rightarrow L_3$, is too weak to show much structure (see Note, p. 1936).

It remains to dispose of the 3.4-ev edge in Si. The only transitions are $\Gamma_{25'} \rightarrow \Gamma_{15}$ or $\Gamma_{2'}$. Tauc's data¹⁴ shows that this edge extrapolates to 2.8 ev in Ge. Thus it is probably $\Gamma_{25'} \rightarrow \Gamma_{15}$, and that $\Gamma_{2'}$ and Γ_{15} are almost degenerate. The $E(k)$ curves may then be quite complicated and a strong edge may result from transitions near $k=0$.

The curves of Fig. 3 are also quite suggestive in connection with the pressure dependence of band edges in Si and Ge. According to Paul,²⁵ the variations of energy (relative to $\Gamma_{25'}$) of L_1 , $\Gamma_{2'}$, and X_1 are 5, 12, and -1 in units of 10^{-12} ev dyne $^{-1}$ cm 2 in Ge. Thus X_1 stays about the same in going from Ge to Si, as indicated in Fig. 3, and L_1 and $\Gamma_{2'}$ both rise, the latter about twice as fast. That other factors than V_{000} are important follows from the fact that the observed change in lattice constant (-4%) accounts for only one-third of the level shifts of L_1 and $\Gamma_{2'}$.

The new information concerning Si is sketched in Fig. 6. The bands near $\Gamma_{2'}$ and Γ_{15} may be quite involved; in the absence of further information concerning the $\Gamma_{2'}-\Gamma_{15}$ splitting, we have not attempted to sketch the bands near these levels accurately.

4. OTHER SEMICONDUCTORS

It is by now well known that all III-V semiconductors composed of second-, third-, and fourth-row elements have band structures quite similar to those of Ge and Si. This has been strikingly demonstrated by optical studies²⁶ whose results are shown in Fig. 7. Note that

the spin-orbit splitting of $L_{3'}$ is well resolved. A spin-orbit splitting with two peaks at 3.3 and 3.9 ev has been observed in PbTe.²⁷

Ehrenreich²⁸ has pointed out that the effective mass m_c of the conduction band level $\Gamma_{2'}$ is given by

$$\frac{m}{m_c} = 1 + \left[\frac{E_0 - E_1}{E_0 + \Delta/3 - E_1} \right] F. \quad (4.1)$$

The factor in brackets in (4.1) corrects for the effect of spin-orbit splitting Δ . This relation has been verified to 2% accuracy² for Ge. Ehrenreich rewrites (4.1) as

$$\frac{m}{m_c} = \left(\frac{\bar{E}_G}{\bar{E}_p} + 1 \right)^{-1}, \quad (4.2)$$

with $\bar{E}_p = 29$ ev in Ge. For InSb, InAs, GaSb, InP, and GaAs, \bar{E}_p is 20 ev within 10%.

From (3.11) and (4.1), we find that if M_f is the same in Ge and Si, $E_0 - E_1 = 4.8$ ev in Si. If we use the value of (M_f) characteristic of the III-V's (corresponding to $\bar{E}_p = 20$ ev), then $E_0 - E_1 = 3.2$ ev. These values bracket the estimates of Sec. 3.

We note that the approximate constancy of E_p for the III-V's confirms the remarks of Sec. 2 concerning the relative accuracy of matrix elements and energy gaps, since the latter vary by almost a factor of 10 in these crystals. Moreover, heteropolarity effects this result only to second order. Since the homopolar (symmetric about center of unit cell) potential gives $\Gamma_{25'}$ even, $\Gamma_{2'}$ odd, the heteropolar potential of order ϵ gives

$$M_F^2(V_e + \epsilon V_0) = M_F^2(V_e) + 0(\epsilon^2). \quad (4.3)$$

Taken together with the remarks of Sec. 2, (4.3) provides justification for the remarkable constancy of M_F^2 noted by Ehrenreich.

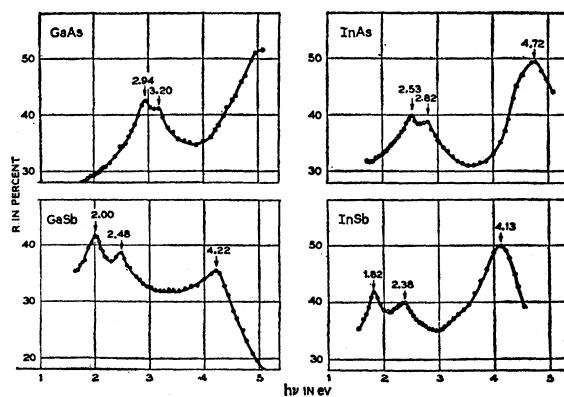


FIG. 7. Optical absorption in the range 2–5 ev for four III-V compounds. Note the similarity of the four curves.

²⁷ S. Yamada, J. Phys. Soc. Japan 15, 1940 (1960). I am grateful to Dr. D. G. Thomas for acquainting me with this work. See also the complete survey of M. Cardona, J. Appl. Phys. 32, 2151 (1961).

²⁸ H. Ehrenreich, Schenectady Conference on Compound Semiconductors [J. Appl. Phys. 32, 2155 (1961)].

²⁵ W. Paul, J. Phys. Chem. Solids 8, 196 (1959).

²⁶ J. Tauc and A. Abraham, see reference 10.

The doubly degenerate level X_1 splits into two levels X_1 and X_3 in III-V compounds. Theory suggests⁸ that the conduction band X_1 - X_3 splitting is small. If the interpretation of edge A in Sec. 3 as $X_4 \rightarrow X_1$ is correct, the edge should be broadened and possibly a splitting of the edge may be seen in III-V compounds. This is indeed the case for the reflectance curves in Fig. 7. For InAs, in addition to the A edge at 4.72 eV ($X_4 \rightarrow X_3$) there is a suggestion of another edge ($X_4 \rightarrow X_1$) near 4.4 eV. Precision measurements of the real and imaginary parts of the index of refraction on etched single crystals might reveal the doublet structure more clearly.

Our assumption that group IV semiconductors fall on the same V_{000} curve can be tested experimentally. From a direct gap $\Gamma_{2'} - \Gamma_{25'} = 0.1$ eV in grey Sn, we anticipate $L_1 = 0.35$ eV. Thus the center of gravity of a strong $L_{3'} \rightarrow L_1$ edge should be at 1.8 eV; allowing for a spin-orbit splitting of 0.6 eV, two peaks at 1.5 and 2.1 eV should be observed. Optical reflection studies on etched single crystals of grey Sn would be of great interest.

Because of the larger spin-orbit interaction, vacuum ultraviolet studies of grey Sn, GaSb, InSb, or PbTe might also be able to resolve the predicted 1:2:1 spin-orbit splitting of peak B , which we have assigned to $L_{3'} \rightarrow L_3$.

Note added in proof. The assignments of levels proposed here have been confirmed by a series of experiments reported by H. Ehrenreich, H. R. Philipp, and J. C. Phillips, Phys. Rev. Letters **8**, 59 (1962). Prior to these experiments many theorists, including the author,

were skeptical of the accuracy of energy-band calculations. It is therefore comforting that the insensitive gaps, especially $\Gamma_{25'} \rightarrow \Gamma_{15}$ and $L_{3'} \rightarrow L_3$, agree so well with theoretical predictions. For spin-orbit effects, see also J. C. Phillips and L. Liu, Phys. Rev. Letters **8**, 94 (1962).

The remarks we have made do not apply to diamond. Because there are no p states in the carbon core, p states see a much larger "effective potential" than s states in diamond. The calculated band structure⁷ predicts a strong $L_{3'} \rightarrow L_1$ absorption edge at 13.6 eV. Philipp and Taft²⁹ have observed a strong edge at about 12 eV, in good agreement with the predicted value.

Another excellent test of the categorical classification given here should be furnished by the ultraviolet reflection spectra of semiconductors which crystallize in both zinc-blende and wurtzite structures. In the wurtzite structure, some rearrangement of levels, as well as additional splittings and polarization effects, should be observed. By correlating the results with those from the same crystal in the zinc-blende form, one should obtain decisive evidence for the band structure of all tetrahedrally coordinated semiconductors.

ACKNOWLEDGMENTS

It is a pleasure to acknowledge the receipt of preprints from Professor J. Tauc, Dr. F. Herman, and Dr. H. Ehrenreich. I am especially grateful to Dr. J. C. Hensel for acquainting me with his results before publication.

²⁹ H. R. Philipp (private communication).